Macromolecules

Article

Cite This: Macromolecules 2017, 50, 9239−9248

Primary Alkylphosphine−Borane Polymers: Synthesis, Low Glass Transition Temperature, and a Predictive Capability Thereof

Hamish Cavaye,[†] Francis Clegg,[‡] Peter J. Gould,[§] Melissa K. Ladyman,[†] Tracey Temple,[†] and Eleftheria Dossi*[,†]

[†]Centre for Defence Chemistry, Cranfield University, Defence Academy of United Kingdom, Shrivenham SN6 8LA, U.K.

[‡]Materials and Engineering Research Institute, Sheffield Hallam University, City Campus, Howard Street, Sheffield S1 1WB, U.K.

[§]QinetiQ, B240, Bristol Business Park, Coldharbour Lane, Bristol BS16 1FJ, U.K.

Supporting Information

ABSTRACT: With a multitude of potential applications, poly(phosphine−borane)s are an interesting class of polymer comprising main-group elements within the inorganic polymer backbone. A new family of primary alkylphosphine−borane polymers was synthesized by a solvent-free rhodium-catalyzed dehydrocoupling reaction and characterized by conventional chemicophysical techniques. The thermal stability of the polymers is strongly affected by the size and shape of the alkyl side chain with longer substituents imparting greater stability. The polymers show substantial stability toward UV illumination and immersion in water; however, they undergo a loss of alkylphosphine units during thermal degradation. The polymers exhibit glass transition temperatures (T_g) as low as −70 °C. A group interaction model (GIM) framework was developed to allow the semiquantitative prediction of T_g values, and the properties of the materials in this study were used to validate the model.

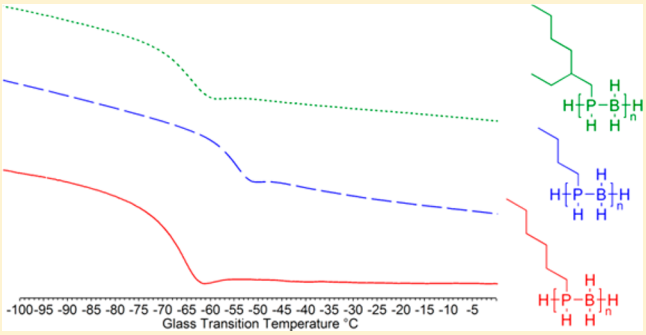

INTRODUCTION

The vast majority of polymer science comprises materials with carbon-based structures. Polymers based on main group elements are of considerable interest thanks to their wide-ranging chemical, thermal, and mechanical properties.[1−4] Much of the research in this field has focused on silicon-based polymers including but not limited to poly(siloxanes)[5−7] and poly(silanes).[8,9] Other more recent areas of interest have included polymers based on elements such as phosphorus,[10−12] sulfur,[13−15] tin,[16,17] and boron.[18,19] One interesting class of boron-containing polymers are the poly(phosphine−borane)s, $[RR'P{\cdot}BH_2]_n$, which have shown potential use in lithography[20,21] and may be useful as pre-ceramic materials.[22] Polymers containing phosphorus or boron have also been shown to be of interest as flame-retardant materials.[23,24]

Poly(phosphine−borane)s contain alternating P and B atoms along the backbone of the polymer chain, which are valence isoelectronic with an all carbon C−C chain, e.g., in a poly(olefin).[25] Work toward synthesizing phosphine−borane adducts and oligomers began during the 1940s and 1950s;[26−28] however, it was not until the late 1990s and early 2000s that reliable methods of forming and characterizing the polymeric materials were presented.[29,20] Since then, a number of different poly(phosphine−borane)s have been reported with a variety of side chains attached to the P atom along the polymer backbone (Figure 1). These side chains include aryl rings (e.g., PBPPB and PDPPB),[21,22,29−31] fluorinated electron-withdrawing groups,[20] and metallocenes;[32] however, there are only a very limited number of studies that describe phosphine−boranes with simple alkyl side chains (e.g., PiBPB and PtBPB).[22,30,33,34]

While the synthesis of poly(phosphine−borane)s has already been studied, theoretical examinations of these materials have not been reported. Group interaction modeling (GIM) is a well-established theoretical framework used to rapidly and reliably predict the properties of polymers as a function of molecular structure.[35] GIM uses a mean-field potential function approach to relate the interactions between defined groups of atoms in a polymer with its thermomechanical properties, e.g., glass transition temperature (T_g). T_g is an important property of polymeric materials as it often defines the temperature range over which the material can be used for a given purpose. As such, polymers with particularly low or high T_g values are highly sought after in order to obtain materials suitable for use at either low or high temperatures, respectively. Polymers exhibiting low T_g values can be important for binding agents, flexible sealants, and rubbers.[36−38]

While GIM is primarily utilized in the prediction of properties of carbon-based polymers,[35] there have been no

Received: September 19, 2017
Revised: November 14, 2017
Published: November 30, 2017

DOI: 10.1021/acs.macromol.7b02030
Macromolecules 2017, 50, 9239−9248

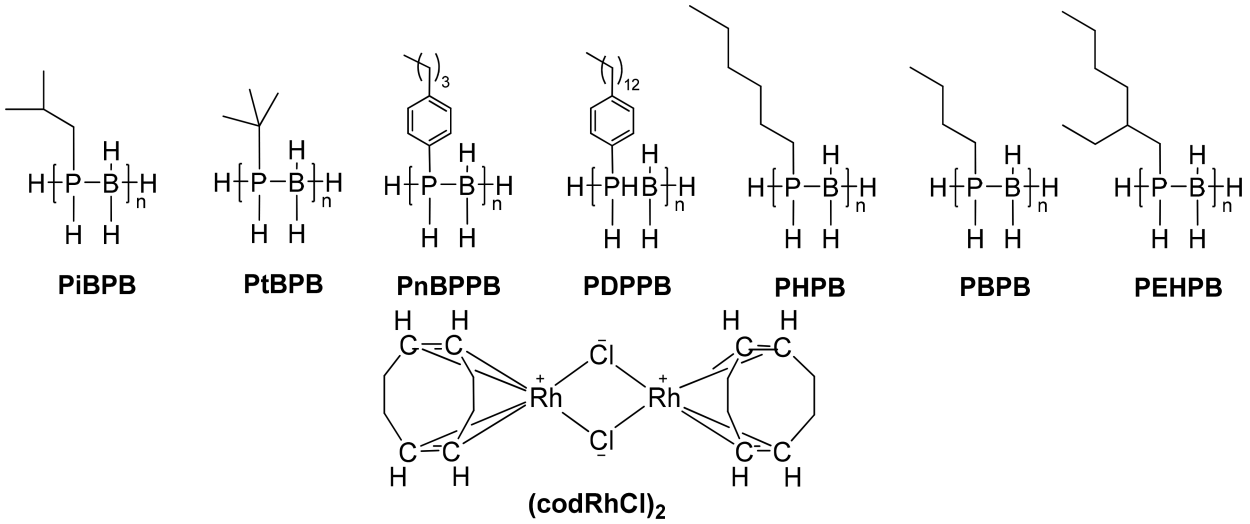

Figure 1. Phosphine–borane polymers from the literature (PiBPB, PtBPB, PnBPPB, PDPPB) and this work (PHPB, PBPB, PEHPB) and the rhodium polymerization catalyst $(codRhCl)_2$.

studies reported that use GIM with main group polymers. Whenever a theoretical technique is expanded to include new classes of materials it is vital to validate the model with experimental data.

In this study the synthesis, characterization, and thermal stability of a new family of primary alkylphosphine–borane polymers are reported (Figure 1). These are the first phosphine–borane polymer derivatives comprising a single primary alkyl chain on the phosphorus. The side groups were chosen in order to examine the effect of different linear alkyl substituents on the thermal properties of poly(phosphine–borane)s. It was believed that such side chains would produce materials with very low glass transition temperatures. As such, these materials were also chosen as suitable candidates for the experimental validation of a GIM analysis of polymers containing P and B in the main chain.

EXPERIMENTAL SECTION

General Methods. All reactions were performed under dry nitrogen unless otherwise specified. Reaction work-ups and purifications were performed in air. Commercial reagents and solvents were used as received. Bis(diethylamino)chlorophosphine (**1**) was prepared following the procedure reported in the literature.[39]

Nuclear magnetic resonance (NMR) spectra were recorded on a Bruker Ascend 400 MHz with a BBFO probe in deuterated chloroform solution with TMS as an internal reference. ^{11}B spectra were processed with a backward linear prediction, real data (LPbr), in order to reduce contributions to the spectra from boron in the NMR sample tubes. Chemical shifts (δ) are given in ppm. Coupling constants (J) are quoted to the nearest hertz (Hz). Peak multiplicities are described in the following way: singlet (s), doublet (d), triplet (t), multiplet (m), doublet of multiplets (dm), broad (br). Infrared (IR) transmission spectra were recorded as neat samples on a Bruker Alpha in diamond attenuated total reflection (ATR) mode. Peaks are defined as weak (w), medium (m), strong (s), or shoulder (sh). Differential scanning calorimetry (DSC) was recorded on a Mettler Toledo DSC 822 using heating and cooling rates of 10 °C min^{-1} and a flow of dry nitrogen unless otherwise specified. Thermogravimetric analysis (TGA) was recorded on a Mettler TG-50 using a heating rate of 10 °C min^{-1} unless otherwise specified. Decomposition temperatures (T_{dec}) are reported for the temperature corresponding to a 5% loss of mass at the aforementioned heating rate. Rheology: rotational (controlled shear rate) experiments were performed using an Anton Paar Physica MCR301 rheometer and Rheoplus/32 software (version 3.40). A 20 mm parallel plate–plate configuration was used with 1 mm gap. Shear rates were increased from 0.01 to 100 s^{-1} while maintaining the sample at 25 °C. Headspace-GCMS was performed using a PerkinElmer Clarus 500 gas chromatograph and mass spectrometer with Turbomass (Version 5.4.2.1617) and NIST mass spectral search program (Version 2.0d) software. Combined TGA and automated thermal desorption (ATD)-GCMS analysis was performed using a NETZSCH 409PG Luxx simultaneous thermal analyzer, a PerkinElmer Turbomatrix 350 ATD, and the same GCMS system used for headspace analysis. Gases evolved from the TGA were trapped using Tenax TA sorbent tubes and subsequently desorbed using the ATD and passed through the GC to be separated and then detected by the MS. Gel permeation chromatography (GPC) measurements were performed in tetrahydrofuran (THF) at 35 °C, using Agilent PLgel 10 μm mixed B columns and Agilent polystyrene calibration kit (M_w 500–6.9 × 10^6).

Synthesis. *Chloro(1,5-cyclooctadiene)rhodium(I) Dimer.* The rhodium catalyst was prepared following the procedure reported in the literature,[40] and the product was isolated as a bright orange solid in quantitative yield, 0.78 g. ^{1}H NMR (400 MHz, $CDCl_3$): δ = 4.22 (4H, s), 2.45–2.55 (4H, m), and 1.77 ppm (4H, m). IR: ν_{max} = 2987 (w), 2933 (m), 2909 (m), 2865 (m), 2825 (m), 1466 (w), 1422 (w), 1321 (m), 1298 (m), 1210 (m), 1171 (w), 993 (m), 959 (st), 865 (m), 814 (st), 774 (m), and 689 cm^{-1} (w).

*Alkyldichlorophosphine [$RPCl_2$] (**2a–c**) General Method.* Example quantities given for **2a**: bis(diethylamino)chlorophosphine (**1**) (11.4 g, 54.3 mmol, 1 equiv) was dissolved in dry diethyl ether (80 mL) in predried glassware with an overhead mechanical stirrer under nitrogen. The reaction vessel was cooled with a dry ice/acetone bath. Alkyllithium solution (24.8 mL, 2.3 M in hexanes, 1.05 equiv) was diluted in dried diethyl ether (60 mL) and then added to the stirring reaction over 15 min. The reaction was stirred for a further 15 min, then the cold bath was removed, and the reaction was stirred for a further 2 h at room temperature. NMR analysis of an aliquot of the reaction mixture showed all of the starting material had been consumed, and the reaction was again cooled with a dry ice/acetone bath. Hydrogen chloride solution (122 mL, 2.0 M in diethyl ether, 4.5 equiv) was then added to the stirring solution over 15 min. The reaction was stirred for a further 1 h, then the cold bath was removed, and the mixture allowed to warm to room temperature before stirring for another 18 h. The crude product was filtered, and dry diethyl ether (250 mL) was used to wash the solids. The solvent was evaporated under reduced pressure to afford product **2a** as a clear, colorless oil.

*n-Hexyldichlorophosphine (**2a**).* 9.12 g (90% yield). ^{1}H NMR (400 MHz, $CDCl_3$): δ = 2.29–2.37 (2H, m), 1.66–1.72 (2H, m), 1.40–1.50 (2H, m), 1.25–1.38 (4H, m), and 0.90 ppm (3H, m, J_{H-H} = 6

DOI: 10.1021/acs.macromol.7b02030
Macromolecules 2017, 50, 9239–9248

Scheme 1. Synthesis of Phosphine−Borane Adduct Monomers

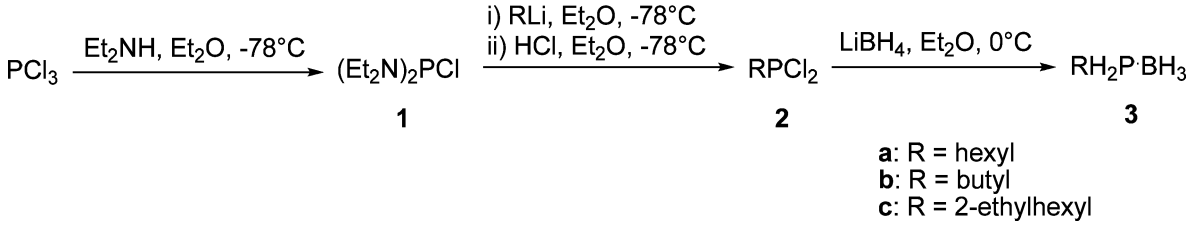

Hz). $^{13}C\{^1H\}$ NMR (101 MHz, $CDCl_3$): δ = 43.3 (d, J_{C-P} = 44 Hz), 31.4 (s), 29.9 (d, J_{C-P} = 10 Hz), 23.1 (d, J_{C-P} = 15 Hz), 22.4 (s), and 14.0 ppm (s). $^{31}P\{^1H\}$ NMR (162 MHz, $CDCl_3$): δ = 196 ppm (s).[41]

*n-Butyldichlorophosphine (**2b**).* 3.50 g (90% yield). ^1H NMR (400 MHz, $CDCl_3$): δ = 2.29−2.37 (2H, m), 1.64−1.71 (2H, m), 1.45−1.51 (2H, m), and 0.97 ppm (3H, m, J_{H-H} = 8 Hz). $^{13}C\{^1H\}$ NMR (101 MHz, $CDCl_3$): δ = 42.99 (d, J_{C-P} = 44 Hz), 25.16 (d, J_{C-P} = 14 Hz), 23.46 (d, J_{C-P} = 11 Hz), and 13.71 ppm (s). $^{31}P\{^1H\}$ NMR (162 MHz, $CDCl_3$): δ = 196 ppm (s).

*2-(Ethylhexyl)dichlorophosphine (**2c**).* 7.45 g (quant). ^1H NMR (400 MHz, $CDCl_3$): δ = 2.36 (2H, dd, J_{H-H} = 7 and 14 Hz), 1.70−1.80 (1H, m), 1.20−1.52 (8H, m), and 0.80−0.97 ppm (6H, m). $^{13}C\{^1H\}$ NMR (101 MHz, $CDCl_3$): δ = 49.4 (d, J_{C-P} = 46 Hz), 35.7 (d, J_{C-P} = 11 Hz), 33.9 (d, J_{C-P} = 8 Hz), 28.5 (s), 27.2 (d, J_{C-P} = 8 Hz), 22.8 (s), 14.0 (s), and 10.6 ppm (s). ^{31}P NMR (162 MHz, $CDCl_3$): δ = 198 ppm (q, J_{P-H} = approximately 13 Hz). $^{31}P\{^1H\}$ NMR (162 MHz, $CDCl_3$): δ = 198 ppm (s).

*Alkylphosphine−Borane Adduct [R(H$_2$)P·BH$_3$] (**3a−c**) General Method.* Example quantities given for **3a**: a slurry of lithium borohydride (360 mg, 16.5 mmol, 2.05 equiv) in dry diethyl ether (20 mL) stirred by a magnetic stirrer was placed under dry nitrogen and cooled in a salt/ice/water bath. A solution of alkyldichlorophosphine (**2a−c**) (1.40 g, 7.5 mmol, 1 equiv) in dry diethyl ether (15 mL) was then added to the slurry over 20 min. The reaction was stirred for a further 20 min before the cold bath was removed, and the mixture was stirred for 21 h at room temperature to reach completion. The solvent was removed under reduced pressure to afford a crude mixture of lithium chloride and a colorless oil. The oil was redissolved in hexane (30 mL) and filtered. The solids were washed with further hexane (20 mL), and the combined organic fractions evaporated under reduced pressure to afford the product as a clear, colorless oil.

*n-Hexylphosphine−Borane Adduct (**3a**).* 890 mg (90% yield). ^1H NMR (400 MHz, $CDCl_3$): δ = 4.50 (2H, dm, J_{H-P} = 350 Hz), 1.77−1.85 (2H, m), 1.57−1.60 (2H, m), 1.36−1.45 (2H, m), 1.36−1.25 (4H, m), 0.88 (3H, t, J_{H-H} = 7 Hz), and 0.61 ppm (3H, br q, J_{H-B} = approximately 92 Hz). $^{13}C\{^1H\}$ NMR (101 MHz, $CDCl_3$): δ = 31.2 (s), 29.9 (d, J_{C-P} = 10 Hz), 26.5 (d, J_{C-P} = 5 Hz), 22.4 (s), 16.5 (d, J_{C-P} = 36 Hz), and 14.0 ppm (s). ^{31}P NMR (162 MHz, $CDCl_3$): δ = −52.2 ppm (br t, J_{P-H} = 350 Hz). $^{31}P\{^1H\}$ NMR (162 MHz, $CDCl_3$): δ = −52.2 ppm (q, J_{P-B} = approximately 44 Hz). ^{11}B NMR (128 MHz, $CDCl_3$): δ = −42.5 ppm (dq, J_{B-H} = 99 Hz, J_{B-P} = 40 Hz); mp (DSC) −49 °C.

*n-Butylphosphine−Borane Adduct (**3b**).* 538 mg (82% yield). ^1H NMR (400 MHz, $CDCl_3$): δ = 4.52 (2H, dm, J_{H-P} = 355 Hz), 1.78−1.88 (2H, m), 1.57−1.67 (2H, m), 1.41−1.49 (2H, m), 0.92 (3H, t, J_{H-H} = 8 Hz), and 0.62 ppm (3H, br q, J_{H-B} = approximately 100 Hz). $^{13}C\{^1H\}$ NMR (101 MHz, $CDCl_3$): δ = 28.6 (d, J_{C-P} = 5 Hz), 23.4 (d, J_{C-P} = 11 Hz), 16.2 (d, J_{C-P} = 36 Hz), and 13.5 ppm (s). ^{31}P NMR (162 MHz, $CDCl_3$): δ = −52.2 ppm (br t, J_{P-H} = 385 Hz). $^{31}P\{^1H\}$ NMR (162 MHz, $CDCl_3$): δ = −52.2 ppm (q, J_{P-B} = approximately 38 Hz). ^{11}B NMR (128 MHz, $CDCl_3$): δ = −42.5 ppm (dq, J_{B-H} = 100 Hz, J_{B-P} = 38 Hz); mp (DSC) < −130 °C.

*2-(Ethylhexyl)phosphine−Borane Adduct (**3c**).* 5.41 g (quant), with some remaining very fine white solids still present. ^1H NMR (400 MHz, $CDCl_3$): δ = 4.50 (2H, dm, J_{H-P} = 360 Hz), 1.77−1.84 (2H, m), 1.62−1.72 (1H, m), 1.21−1.46 (8H, m), 0.87−0.91 (6H, m), and 0.62 ppm (3H, br q, J_{H-B} = approximately 100 Hz). $^{13}C\{^1H\}$ NMR (101 MHz, $CDCl_3$): δ = 36.8 (d, J_{C-P} = 5 Hz), 33.1 (d, J_{C-P} = 7 Hz), 28.5 (s), 26.3 (d, J_{C-P} = 7 Hz), 22.8 (s), 20.7 (d, J_{C-P} = 34 Hz), 14.0 ppm (s), and 10.5 (s). ^{31}P NMR (162 MHz, $CDCl_3$): δ = −60.4 ppm (br t, J_{P-H} = 360 Hz). $^{31}P\{^1H\}$ NMR (162 MHz, $CDCl_3$): δ = −60.2 ppm (q, J_{P-B} = approximately 40 Hz). ^{11}B NMR (128 MHz, $CDCl_3$): δ = −42.2 ppm (dq, J_{B-H} = 99 Hz, J_{B-P} = 40 Hz).

Alkylphosphine−Borane Polymer [RHPBH$_2$]$_n$ (PHPB, PBPB, PEHPB) General Method. Example quantities are given for PHPB. Other reactions were performed using varying loadings of the catalyst. Alkylphosphine−borane adduct (**3a−c**) (400 mg, 3.0 mmol) was placed under nitrogen in a predried Schlenk tube. Upon addition of chloro(1,5-cyclooctadiene)rhodium(I) dimer (14.9 mg, 2 mol % Rh(I)) to the stirring monomer the mixture turned a dark color, and evolution of gas was observed. The reaction was stirred and placed into an oil bath heated to 120 °C and then left stirring at this temperature for 45 min−22 h. After cooling to room temperature, tetrahydrofuran (2 mL) was added to the reaction mixture, which became soluble with gentle warming and stirring. The solution was precipitated from a vigorously stirring mixture of water/isopropanol (1:1 v/v) for PHPB and PBPB or from water for PEHPB. The supernatant liquid was decanted, and the remaining viscous oil was washed with methanol (15 mL) and dried under reduced vacuum to afford the product PHPB.

PHPB: 310 mg (80% yield). ^1H NMR (400 MHz, $CDCl_3$): δ = 3.80 (1H, br d, J_{H-P} = 340 Hz), and 0.7−2.0 ppm (15H, br m). $^{13}C\{^1H\}$ NMR (101 MHz, $CDCl_3$): δ = 31.5 (s), 30.6 (br), 26.1 (br), 22.6 (s), 20.7 (br), and 14.1 ppm (s). $^{31}P\{^1H\}$ NMR (162 MHz, $CDCl_3$): δ = −55.8 (br), and −60 to −65 ppm (br m). ^{11}B NMR (128 MHz, $CDCl_3$): δ = −35.6 ppm (br). IR: ν_{max} = 2955 (sh), 2923 (st), 2855 (m), 2406 (m), 2367 (m), 1458 (m), 1412 (w), 1378 (w), 1111 (m), 977 (m), 892 (m), 835 (m), 754 (m), and 713 cm^{-1} (st). T_g = −69 °C. T_{dec} = 245 °C (N_2), 256 °C (air).

PBPB: 270 mg (69% yield). ^1H NMR (400 MHz, $CDCl_3$): δ = 3.81 (1H, br dm, J_{H-P} = 340 Hz), and 0.7−2.1 ppm (11H, br m). $^{13}C\{^1H\}$ NMR (101 MHz, $CDCl_3$): δ = 28.2 (s), 24.0 (d), 20.3 (br s), and 13.7 ppm (s). $^{31}P\{^1H\}$ NMR (162 MHz, $CDCl_3$): δ = −56.0 (br m), and −60.0 to −65.0 ppm (br m). ^{11}B NMR (128 MHz, $CDCl_3$): δ = −36.2 ppm (br). IR: ν_{max} = 2956 (st), 2928 (st), 2870 (m), 2403 (m), 2365 (st), 1462 (m), 1411 (w), 1378 (w), 1343 (w), 1299 (w), 1215 (w), 1187 (w), 1111 (m), 1096 (m), 1066 (m), 988 (m), 931 (m), 892 (m), 836 (st), and 714 cm^{-1} (st). T_g = −58 °C. T_{dec} = 147 °C (N_2).

PEHPB: 225 mg (46% yield). ^1H NMR (400 MHz, $CDCl_3$): δ = 3.0−5.5 (1H, br m), and 0.7−2.1 ppm (19H, br m). $^{13}C\{^1H\}$ NMR (101 MHz, $CDCl_3$): δ = 35.9 (br s), 33.2 (br d), 28.5 (br s), 26.3 (br d), 23.1 (br s), ∼20 (very weak br), 14.2 (s), and 10.4 ppm (s). ^{31}P NMR (162 MHz, $CDCl_3$): δ = −69.9 (br) and −96.0 ppm (br). $^{31}P\{^1H\}$ NMR (162 MHz, $CDCl_3$): δ = −63.0 (br), −65.0 to −75.0 (br m), and −97.0 ppm (br). ^{11}B NMR (128 MHz, $CDCl_3$): δ = −35.3 ppm (br). IR: ν_{max} = 2957 (s), 2924 (s), 2871 (sh), 2857 (m), 2364 (br, m), 1459 (m), 1409 (w), 1379 (m), 1260 (w), 1213 (w), 1176 (w), 1111 (m), 1061 (w), 931 (m), 796 (m), 752 (m), 695 (m), and 579 (w). T_g = −66 °C. T_{dec} = 181 °C (N_2).

RESULTS AND DISCUSSION

Monomer Synthesis and Characterization. Synthesis of the alkyl-substituted phosphine−borane adduct monomers was performed using the steps outlined in the literature and shown in Scheme 1.[22] This synthetic route avoids the production of free, potentially pyrophoric alkylphosphines by directly

DOI: 10.1021/acs.macromol.7b02030
Macromolecules 2017, 50, 9239−9248

converting the alkyldichlorophosphines (compounds **2a–c**) to alkylphosphine–borane adducts in a single step.

First, phosphorus trichloride is reacted with 2 equiv of diethylamine to afford bis(diethylamino)chlorophosphine **1**. A further 2 equiv of diethylamine is necessary to react with the hydrogen chloride that is formed, causing diethylammonium chloride to precipitate as a byproduct. Samples of compound **1** were then separately reacted with three different commercially available alkyllithium reagents: *n*-hexyllithium, *n*-butyllithium, and 2-(ethylhexyl)lithium. This second step of the synthetic scheme is better described as a two-step, one-pot reaction. After the chloride functionality in compound **1** is replaced by the alkyl anion, an excess of hydrochloric acid is then used to convert the diethylamine groups back to chlorides, thus affording compounds **2a–c**, which were isolated with traces (<2%) of oxidized side-products (NMR spectra available in the Supporting Information). Finally, the alkyldichlorophosphine compounds **2a–c** were each separately reacted with 2 equiv of lithium borohydride to form *n*-hexylphosphine–borane (**3a**), *n*-butylphosphine–borane (**3b**), and 2-(ethylhexyl)phosphine–borane (**3c**), respectively. It is believed that the traces of oxidized materials used in this reaction were first reduced before forming the adducts as compounds **3a–c** were isolated without impurities.

All three monomers **3a–c** were characterized using the four different NMR-active nuclei present in the samples: ^{1}H, ^{13}C, ^{31}P, and ^{11}B. They were shown to have spectra consistent with other phosphine–borane adducts that are reported in the literature (figures available in the Supporting Information).[27] The low-temperature differential scanning calorimetry (DSC) of **3a** was recorded between 25 and −130 °C. Interestingly, the compound showed a cold-crystallization process as seen in Figure 2. No phase transitions are observed during cooling;

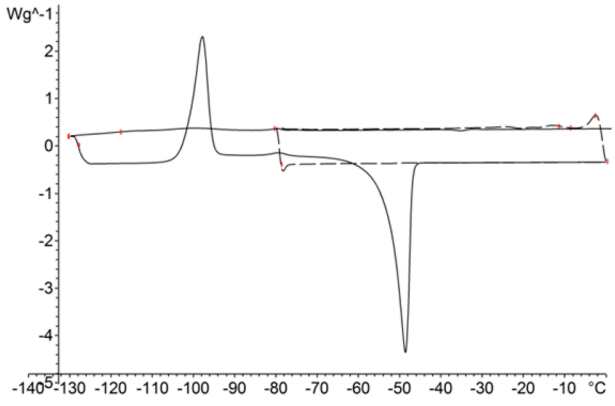

Figure 2. Low-temperature DSC curves for phosphine–borane adduct **3a** showing cold crystallization occurring when **3a** is cooled to below −110 °C (solid line) but not when it is only cooled to −80 °C (dashed line).

however, during heating there is a crystallization at −98 °C followed by a melting at −49 °C. This process was shown to be repeatable, and when the compound was cooled to −80 °C before warming again, then no phase changes were observed at all. When the same measurement was performed for **3b**, with the shorter butyl side chain, no phase transitions at all were observed as low as −130 °C.

Polymer Synthesis. When heated in the presence of an appropriate catalyst, phosphine–borane adducts undergo a dehydrocoupling polymerization reaction to form linear poly(phosphine–borane)s with alternating phosphorus and boron atoms in the main chain (Scheme 2).[33,42] The

Scheme 2. Polymerization Reaction of Phosphine–Boranes

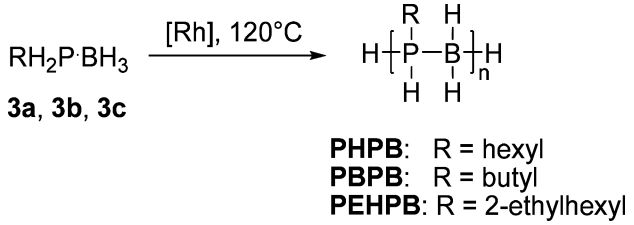

polymerization of phosphine–borane adducts such as **3a–c** is catalyzed by the di-μ-chloro-bis(η^4-1,5-cyclooctadiene)-dirhodium(I) catalyst [$(codRhCl)_2$] shown in Figure 1. This catalyst was prepared using a literature method from rhodium(III) chloride and 1,5-cyclooctadiene.[40] The rhodium(III) chloride is dissolved in deoxygenated ethanol–water (5:1) before 1,5-cyclooctadiene is added, and the reaction refluxed until the orange-yellow rhodium(I) catalyst precipitates.

A previous report of the polymerization of aryl-substituted phosphine–borane adducts with $(codRhCl)_2$ showed some success in refluxing toluene via what was believed to be a step growth mechanism.[30] Initial attempts to polymerize **3a** in toluene solution were unsuccessful and afforded only unreacted starting material. It was reported in the literature that inclusion of electron-withdrawing substituents on the phosphorus atom of the phosphine–borane adduct causes the phosphine protons to become more acidic, thus leading to an increase in the reactivity toward dehydrocoupling.[20,43] The monomer units **3a–c** comprise positively inductive alkyl side chains, and it is believed that this is why no reaction at all was observed when the polymerization was performed in toluene solution. The polymerizations were achieved by simple addition of the catalyst to neat monomer without any solvent (Scheme 2). Upon mixing $(codRhCl)_2$ with the monomers **3a–c** at room temperature, there was an immediate change in color of the reaction mixture from the yellow-orange of the catalyst to a darker brown, which is believed to be related to the formation of the active catalytic species; the depth of the color was related to the quantity of catalyst being used in the reaction. As the polymerization reactions progressed, bubbles were visibly formed as the dehydrogenation took place. Over time the mixtures became notably more viscous especially when attempting to produce high molecular weight products or when using high catalyst loadings.[30,31] A very high catalyst loading (>5%) or longer reaction times led to poorly soluble products with very high dispersities. In order to obtain soluble products with reasonably low polydispersity indices (PDIs), the polymerizations of **3a–c** were monitored visually, and when the increased viscosity showed that mixing had become poor, the reactions were stopped by cooling to room temperature. As can be seen in Table 1, the greater the loading of catalyst, the less time was needed before the mixture became very viscous and the reaction was stopped. The newly formed polymers were then dissolved in small quantities of tetrahydrofuran (THF), ca. 200–300 mg mL^{-1}, before precipitating from a 50/50 water/2-propanol mixture for PHPB and PBPB or from water in the case of PEHPB. The increased solubility of PEHPB compared to PHPB and PBPB may have been a contributing factor to the lower overall isolated yield for this polymer.

DOI: 10.1021/acs.macromol.7b02030
Macromolecules 2017, 50, 9239–9248

Table 1. Typical Properties of the Phosphine−Borane Polymers PHPB, PBPB, and PEHPB

	[Rh][a] (mol %)	T[b]	isolated yield (%)	M_w[c]	M_n[c]	PDI[d]	T_g (°C)
PHPB	0.5	22 h	80	19500	8800	2.2	−65
PHPB	2.0	4 h	92	9050	3750	2.4	−68
PHPB	5.0	45 min	81	4650	2550	1.8	−65
PBPB	2.0	2 h	69	2500	1700	1.5	−58
PEHPB	2.0	4 h	46	3650	3120	1.2	−66

[a]$(codRhCl)_2$ catalyst loading. [b]Duration of the polymerization reaction. [c]Molecular weights determined by GPC comparison to polystyrene standards. [d]Polydispersity index (M_w/M_n).

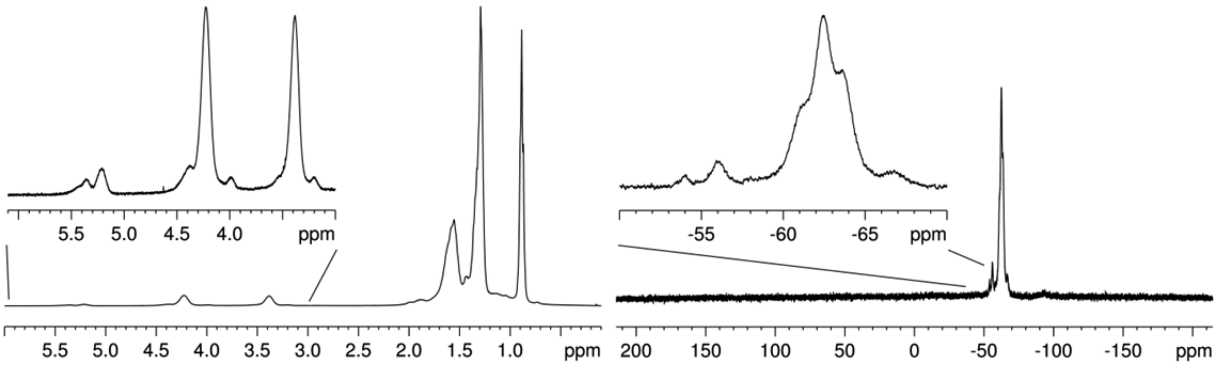

Figure 3. ^1H (left) and $^{31}P\{^1H\}$ (right) NMR spectra for a sample of PHPB.

Polymer Characterization. As for the monomeric units, the three polymers PHPB, PBPB, and PEHPB were characterized using all four NMR-active nuclei. The $^{31}P\{^1H\}$ NMR spectra show evidence of an isotactic polymer being produced as has been discussed for similar compounds previously.[34] The NMR spectra recorded for the samples in this study showed additional peaks, found in the region of 4.0−5.5 and −56 ppm in the ^1H NMR and $^{31}P\{^1H\}$ NMR spectra, respectively (Figure 3), when compared to other phosphine−borane polymers in the literature.[21,27,29,30,34] These peaks have been attributed to the phosphine end-group of the polymers. This assignment is based on two pieces of evidence. First, the small additional peaks are close in position to the phosphine peaks of the monomeric units. Second, for different samples of PHPB the relative intensity of the additional peaks changes with the molecular weight of the sample; longer polymer chains show less intense additional peaks. An attempt was made to use the integrated intensity of these peaks as an estimate of molecular weight for the polymer samples; however, due to the thermal stability issues discussed below, quantitative analysis was not found to be possible. It is believed that the overall lower molecular weights of the samples in this study (also discussed below) led to these peaks becoming more pronounced than for samples previously reported in the literature. There were no additional peaks observed in the ^{11}B NMR spectra; however, this was to be expected as the ^{11}B signal for the polymers was very broad and without structure.

All of the samples were highly soluble in common organic solvents such as THF, diethyl ether, chloroform, and acetone but were insoluble in alcohols and water. The exception to this was the sample of PEHPB, which showed some level of solubility in 2-propanol.

The polymer samples synthesized in this study were examined by gel permeation chromatography (GPC) in THF and compared with poly(styrene) standards. It should be noted that due to the poor mixing mentioned in the previous section, molecular weights of samples varied even when catalyst loading and reaction duration were unchanged. As such, typical results of these experiments are shown in Table 1. In this case a typical result is deemed to be close to the average of all results measured during the study. It is however still clear to see that polymerization reactions with low catalyst loadings led to products with a higher molecular weight than those reactions using high catalyst loadings, which is consistent with the polymerization proceeding via a step growth mechanism. The highest molecular weight sample of PHPB formed in this study used 0.5 mol % catalyst loading and was heated for 22 h. This resulted in a polymer with M_w 19 500, M_n 8800, and a polydispersity index (PDI) of 2.2. For PHPB a higher catalyst loading led to shorter chains, and this is expected to hold true for the other polymers but was not tested. In general, all of the samples showed low PDIs when compared to similar compounds in the literature,[29,30,32,33] ranging from 1.2 to 2.4, which is likely due to the relatively low molecular weights.

Rotational (controlled shear rate) rheology was performed at 25 °C on a sample of PHPB from a polymerization using 2 mol % catalyst loading.[44] The results demonstrated that the polymer has ideal viscous behavior, i.e., Newtonian (Figure S10, Supporting Information). An average viscosity of 10.51 ± 0.2 Pa·s was obtained from all the data points over the whole shear rate range.

Measurement and Prediction of Glass Transition Temperature. The glass transition temperature (T_g) values of the three polymers were studied experimentally by DSC under nitrogen. The materials were also investigated theoretically using group interaction modeling (GIM).

Table 1 shows the experimentally determined T_g values for the materials in this study. The different samples of PHPB exhibited very similar T_g values regardless of the catalyst loading and molecular weight. The polymers formed by polymerization with 2 mol % catalyst loading had T_g values of −68, −58, and −66 °C for PHPB, PBPB, and PEHPB, respectively, which are and notably lower than those reported for other poly(phosphine−borane) polymers.[22,31] For example,

DOI: 10.1021/acs.macromol.7b02030
Macromolecules 2017, 50, 9239−9248

the sample of PHPB exhibited a T_g of −65 °C whereas a sample of $[(p\text{-}n\text{BuC}_6\text{H}_4)\text{PH-BH}_2]_n$ with comparable M_w (ca. 20 000 Da) exhibited a T_g of 8 °C. These differences are attributed to the flexibility of the primary alkyl chains that have been used in this work as well as the lack of aryl rings necessary to promote $\pi-\pi$ stacking. This result is consistent with PBPB having the highest T_g of the polymers tested as it has the shortest side chain.

In order to further understand the glassy behavior of these materials and to develop a predictive capability for future molecular design, GIM was employed. GIM uses the intermolecular energy of interacting groups of atoms as a basis for rapidly and simply predicting properties of a polymer as a function of composition and molecular structure.[35] An initial GIM model was refined and validated by comparing literature data for poly(alkylstyrenes) with their predicted values. This first step introduced the empirical observation that polymers comprising side chains longer than eight methylene units in length begin to interact with each other, reducing their mobility. The model was then applied to simple polyolefins, which can be considered to be carbon−carbon analogues of the phosphine−borane polymers in this study (see the Supporting Information for more details of the GIM model). Figure 4 shows the comparison of T_g values predicted by the model with experimental data from the wider literature.

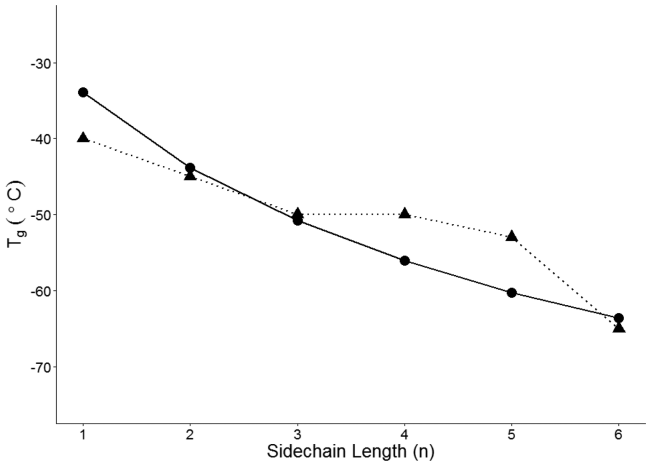

Figure 4. T_g values for polyolefins with varying side chain lengths; n is the number of carbon atoms in the side chain. GIM predicted (solid line, dots) and experimental data (dashed line, triangles) from the literature.

The cohesive energy (E_{coh}) of the model is calculated by group contribution methods.[35] GIM has contribution values for standard groups comprising C, H, N, and O; however, it does not include values for groups comprising P and B. As such, the values were provided by van Krevelen,[45] but it must be noted that values for other groups quoted by van Krevelen are generally higher than for the same groups in GIM. These values were used to adapt the model to include the group contributions from the alternating P and B polymer backbone and can be seen in Table 2.

Table 3 shows the predicted T_g values for poly(alkylphosphine−borane)s compared to experimental results from this study and from the literature. It can be seen that there is reasonable agreement for three of the four materials; the predicted values are within ca. 5 °C of the measured values.

Table 2. Group Contributions to E_{coh} Used in the GIM Model

group	E_{coh} contribution (J/mol)
$-CH_n-$	4500
P	9500
B	14000

Table 3. A Comparison of T_g Values Predicted by GIM and Measured by Experiment

sample	predicted T_g (°C)	measured T_g (°C)
PHPB	−63.4	−68
PBPB	−31.0	−58
PEHPB	−60.4	−66
poly(isobutylphosphine−borane)	+4.4	+5[22]

One explanation for the small deviation would be that the T_g values in this study were measured using DSC. GIM defines the T_g as the temperature at 1 Hz measurement rate and zero pressure of the peak in the loss tangent, which for a homopolymer would equate to the only alpha peak measured in a dynamic mechanical analysis test. There is a larger discrepancy for PBPB, which has a measured T_g value 27 °C lower than the predicted value. This may be in part explained by the low molecular weight for the sample of PBPB (M_w = 2500 g mol^{-1}, Table 1) as GIM assumes an infinite polymer chain. Finally, the largest uncertainty in the prediction comes from the 1-D Debye temperature used for the P−B polymer chain. Further refinement to the model would be highly beneficial, e.g., molecular modeling or direct measurement to obtain accurate group contributions for the P−B backbone. However, the GIM model still offers a very rapid assessment to give semiquantitative information regarding the likely glassy behavior of these materials.

Thermal Stability. Dynamic thermogravimetric analyses (TGA) were performed on PHPB, PBPB, and PEHPB (made using 2 mol % catalyst loading) in a nitrogen gas flow at a heating rate of 10 °C min^{-1}, and the results are shown in Figure 5. The temperature at which each material exhibited a 5% loss of mass (T_{dec}) was 245 °C for PHPB, 147 °C for PBPB, and 181 °C for PEHPB. A previously reported phosphine−borane polymer containing an isobutyl side chain exhibited a T_{dec} of 150 °C,[22] which is in very close agreement with PBPB in this

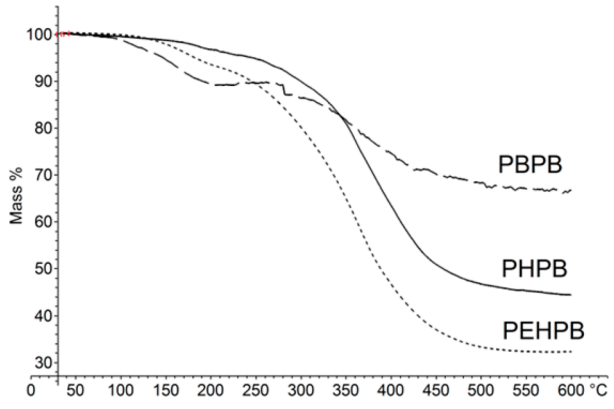

Figure 5. Dynamic TGA measurements of PHPB (solid line), PBPB (dashed line), and PEHPB (dotted line) between 30 and 600 °C at a heating rate of 10 °C min^{-1} under nitrogen flow. All samples were from polymerizations using 2 mol % catalyst loading.

DOI: 10.1021/acs.macromol.7b02030
Macromolecules 2017, 50, 9239−9248

study. These results suggest that the side chain has a pronounced effect on the thermal stability of the polymers with longer side chains leading to higher decomposition temperatures. The shorter *n*-butyl side chain of PBPB is likely to lead to decomposition products that are smaller and more volatile; thus, it is more susceptible to degradation, and this is consistent with it having the lowest T_{dec} of the three polymers tested. It is not immediately obvious what would cause the sample of PEHPB with the 2-(ethylhexyl) side chain to decompose more at a lower temperature than a sample of PHPB. One possible explanation is that the decomposition products of these polymers include the organic side chain. If this is the case, then loss of the bulkier, heavier 2-(ethylhexyl) side chain would lead to a greater reduction in sample mass than loss of an *n*-hexyl side chain. The bulkier side chain may also impart some additional steric stress on the backbone of the polymer, inducing decomposition at a lower temperature for PEHPB than for PHPB. The quantity of pyrolysis residue remaining at the end of the decomposition experiments is proportional to the mass of the side chain as well. That is, PBPB with the shortest side chain leaves the highest percentage of residue and PEHPB with the largest side chain leaves the lowest percentage of residue. This is consistent with the majority of the mass loss during pyrolysis being organic in nature, leaving behind inorganic compounds comprising phosphorus and boron. As mentioned above, poly(phosphine−borane)s have been considered as possible preceramic materials. This work suggests that highly soluble phosphine−boranes can be synthesized with alkyl side chains and that shorter side chains would lead to a greater yield of ceramic mass after pyrolysis.

Further investigations into the stability of PHPB were performed using a sample prepared with 2 mol % catalyst loading. Figure 6 shows the results of isothermal TGA analysis, which examined how mass was lost from a sample of PHPB over a period of 12 h at different temperatures under a stream of nitrogen.

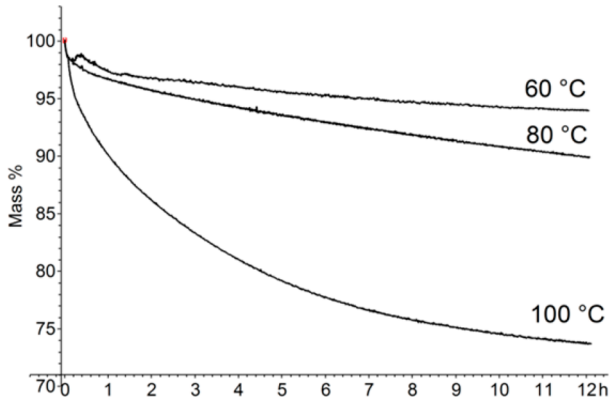

Figure 6. Isothermal TGA of PHPB for 12 h at 60, 80, and 100 °C under a stream of nitrogen.

Mass loss was recorded for samples of PHPB for all temperatures tested; higher temperatures led to a more rapid loss of mass. After 12 h heating at 60 °C the sample had lost 6% of the starting mass, and at 80 °C the sample had lost 10% of the starting mass; however, at 100 °C the sample had lost a rather significant 26% of the starting mass. These losses in mass are too high to be fully accounted for by continued dehydrocoupling within the samples, and therefore some thermal decomposition of the polymer must be occurring. Some preliminary investigations of the mechanism of decomposition were undertaken.

A sample of PHPB was heated at 100 °C for 24 h, and the NMR spectra recorded before and after heating were compared. It is worth noting that these are solution spectra of only the soluble products remaining after heating; however, no significant quantity of insoluble product was observed during the experiments. The majority of the ^{1}H NMR spectrum was unchanged after heating; however, as can be seen in Figure 7, the small peaks around 5.2−5.5 and 4.0−4.5 ppm were notably reduced. The same effect was more pronounced in the ^{31}P{^{1}H} NMR spectrum where the peaks around −55 ppm were significantly reduced as well. All these peaks are attributed to the phosphine end-group of the polymer chains as discussed above. Two possible mechanisms by which the proportion of phosphine end-groups would be reduced in a sample of PHPB are chain extension reactions by further dehydrocoupling or scission of the dative phosphorus−boron bond in the polymer end-group with subsequent release of *n*-hexylphosphine. GPC measurements of the polymer before and after heating showed that the M_w of the sample had increased by 60%, from 4800 to 8300 (PDI increased from 1.8 to 1.9). While this result showed that chain extension must have occurred in the polymer at this temperature, another result consistent with a step growth polymerization mechanism, it has already been mentioned that dehydrocoupling alone could not account for the amount of mass lost. A longer duration experiment involved heating a sample of PHPB at just 40 °C for 7 weeks. During this time the ^{1}H and ^{31}P{^{1}H} NMR spectra showed similar changes to those seen in Figure 7, suggesting that there was a reduction in the proportion of phosphine end-groups even at quite mild temperatures over long periods of time.

To further corroborate the formation of *n*-hexylphosphine upon degradation, headspace-GCMS analysis of the gases extracted from a room temperature sealed vial containing PHPB was performed. Only one significant component was detected in the gas chromatogram, and the associated mass spectrum (Figure 8) indicates a parent ion of mass (m/z = 118) corresponding to *n*-hexylphosphine and a fragmentation pattern to support its presence. It was also of interest to note that the most predominant gas trapped on to the absorbent in the Tenax TA tubes from the exhaust during a TGA analysis at 176 °C (the onset degradation temperature of PHPB; see Figure 5) and subsequently analyzed by ATD-GCMS also showed the same mass spectrum as that observed in the headspace-GCMS, indicating the evolution of *n*-hexylphosphine. Even at 290 °C the same species was dominant, though additional six carbon-containing hydrocarbon species were noted (to a much lesser degree), demonstrating the onset of different degradation pathways at this higher temperature.

Considering all of the results together, it seems most likely that when a sample of PHPB is heated, a combination of two processes occurs: chain extension by further dehydrocoupling and loss of *n*-hexylphosphine from end-group scission. While the chain extension is likely to only be significant at temperatures above 100 °C, the decomposition of the polymer appears to occur to some extent over a wide range of temperatures with higher temperatures leading to more rapid loss of mass.

Finally, samples of PHPB that were exposed to ultraviolet light or immersed in water for 7 weeks at room temperature

DOI: 10.1021/acs.macromol.7b02030
Macromolecules 2017, 50, 9239−9248

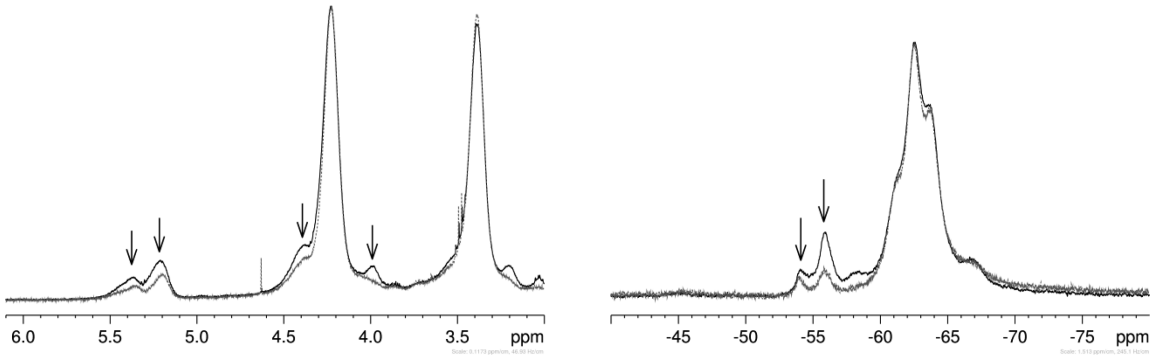

Figure 7. Zoomed regions of the ^{1}H (left) and $^{31}P\{^{1}H\}$ (right) NMR spectra of PHPB before heating (solid black lines) and after heating (dashed gray lines). Arrows denote the peaks that have reduced in intensity after heating.

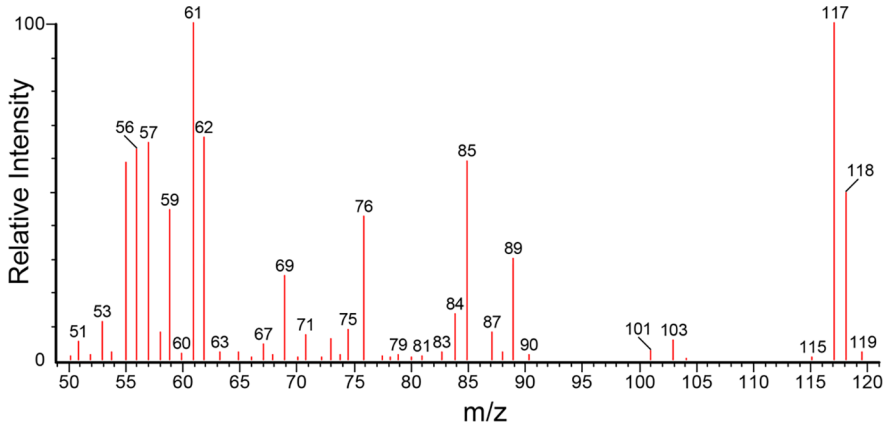

Figure 8. Mass spectrum collected from headspace-GCMS of PHPB. Possible fragmentation assignments include m/z = 118 ($C_6H_{13}P^+H_2$), m/z = 117 ($C_6H_{13}P^+H$), m/z = 103 ($C^+H_2C_4H_8PH_2$), m/z = 89 ($C^+H_2C_3H_6PH_2$), m/z = 85 ($C_5H_{11}C^+H_2$), m/z = 71 ($C_4H_9C^+H_2$), m/z = 61 ($C^+H_2CH_2PH_2$), and m/z = 57 ($C_3H_7C^+H_2$).

showed little or no change in the NMR spectra, demonstrating the stability of the polymer to such environmental conditions.

CONCLUSIONS

A new family of primary alkylphosphine−borane polymers was synthesized by a solvent-free rhodium-catalyzed dehydrocoupling reaction. These polymers exhibit very low glass transition temperatures as low as −70 °C. A GIM framework was developed to allow the semiquantitative prediction of T_g values, and the properties of the materials in this study were used to validate the model. It was found that the size and shape of the alkyl side chain had a pronounced effect on the thermal stability of the polymers as well as the quantity of residue remaining after pyrolysis. A more detailed examination of the thermal stability of poly(*n*-hexylphosphine−borane), PHPB, suggested that the polymers undergo a slow loss of alkylphosphine end-groups at temperatures as low as 40 °C with an increasing rate of decomposition at higher temperatures. Even at room temperature an atmosphere containing primarily alkylphosphine was detected around the polymer sample. In contrast to this, PHPB showed very good stability to immersion in water and exposure to UV irradiation for a number of weeks, suggesting good chemical stability. These highly soluble, low-T_g materials might be useful for low-temperature applications, for lithographic techniques, as solution-processable pre-ceramic compounds, or as flame-retardant materials with tunable degradation temperatures.

ASSOCIATED CONTENT

Supporting Information

The Supporting Information is available free of charge on the ACS Publications website at DOI: 10.1021/acs.macromol.7b02030.

Scheme S1 and Figures S1−S17 (PDF)

AUTHOR INFORMATION

Corresponding Author

*E-mail: e.dossi@cranfield.ac.uk (E.D.).

ORCID

Hamish Cavaye: 0000-0002-3540-0253

Eleftheria Dossi: 0000-0001-6365-8019

Notes

The authors declare no competing financial interest.

ACKNOWLEDGMENTS

This research is part of the "Binders by Design" program which was undertaken through the Weapons Science and Technology Centre (WSTC) and funded by UK Defence Science and Technology Laboratory (DSTL). The authors thank Dr. Nathalie Mai (Cranfield University) for GPC analysis.

REFERENCES

(1) Caminade, A.-M.; Hey-Hawkins, E.; Manners, I. Smart Inorganic Polymers. *Chem. Soc. Rev.* **2016**, *45*, 5144−5146.

DOI: 10.1021/acs.macromol.7b02030
Macromolecules 2017, 50, 9239−9248

(2) Mark, J. E.; Allcock, H. R.; West, R. *Inorganic Polymers*, 2nd ed.; Oxford University Press: New York, 2005.
(3) Leitao, E. M.; Jurca, T.; Manners, I. Catalysis in service of main group chemistry offers a versatile approach to p-block molecules and materials. *Nat. Chem.* **2013**, *5*, 817−829.
(4) Priegert, A. M.; Rawe, B. W.; Serin, S. C.; Gates, D. P. Polymers and the p-block elements. *Chem. Soc. Rev.* **2016**, *45* (4), 922−953.
(5) Zhang, R.; Mark, J. E.; Pinhas, A. R. Dehydrocoupling Polymerization of Bis-silanes and Disilanols to Poly(silphenylenesiloxane) As Catalyzed by Rhodium Complexes. *Macromolecules* **2000**, *33* (10), 3508−3510.
(6) Clarson, S. J.; Semlyen, J. A. *Siloxane Polymers*; Prentice Hall: Eaglewood Cliffs, NJ, 1993.
(7) Clarson, S. J.; Fitzgerald, J. J.; Owen, M. J.; Smith, S. D. *Silicones and Silicone-Modified Materials*; American Chemical Society: Washington, DC, 2000.
(8) Aitken, C. T.; Harrod, J. F.; Samuel, E. Identification of some intermediates in the titanocene-catalyzed dehydrogenative coupling of primary organosilanes. *J. Am. Chem. Soc.* **1986**, *108* (14), 4059−4066.
(9) Miller, R. D.; Michl, J. Polysilane high polymers. *Chem. Rev.* **1989**, *89* (6), 1359−1410.
(10) Rothemund, S.; Teasdale, I. Preparation of polyphosphazenes: a tutorial review. *Chem. Soc. Rev.* **2016**, *45*, 5200−5215.
(11) Allcock, H. R.; Kugel, R. L. Synthesis of High Polymeric Alkoxy- and Aryloxyphosphonitriles. *J. Am. Chem. Soc.* **1965**, *87* (18), 4216−4217.
(12) Allcock, H. R. *Chemistry and Applications of Polyphosphazenes*; Wiley: Hoboken, NJ, 2002.
(13) Chung, W. J.; Griebel, J. J.; Kim, E. T.; Yoon, H.; Simmonds, A. G.; Ji, H. J.; Dirlam, P. T.; Glass, R. S.; Wie, J. J.; Nguyen, N. A.; Guralnick, B. W.; Park, J.; Somogyi, Á.; Theato, P.; Mackay, M. E.; Sung, Y.-E.; Char, K.; Pyun, J. The use of elemental sulfur as an alternative feedstock for polymeric materials. *Nat. Chem.* **2013**, *5*, 518−524.
(14) Steudel, R. The Chemistry of Organic Polysulfanes R−Sn−R (*n* > 2). *Chem. Rev.* **2002**, *102* (11), 3905−3946.
(15) Steudel, R. Sulfur: Organic Polysulfanes. In *Encyclopedia of Inorganic Chemistry*; Wiley: 2007.
(16) Imori, T.; Lu, V.; Cai, H.; Tilley, T. D. Metal-Catalyzed Dehydropolymerization of Secondary Stannanes to High Molecular Weight Polystannanes. *J. Am. Chem. Soc.* **1995**, *117* (40), 9931−9940.
(17) Caseri, W. Polystannanes: processible molecular metals with defined chemical structures. *Chem. Soc. Rev.* **2016**, *45*, 5187−5199.
(18) Kolel-Veetil, M. K.; Keller, T. M. The State of the Art in Boron Polymer Chemistry. In *Macromolecules Containing Metal and Metal-Like Elements*; Wiley: Hoboken, NJ, 2007; Vol. *8*, pp 1−76.
(19) Staubitz, A.; Robertson, A. P. M.; Sloan, M. E.; Manners, I. Amine− and Phosphine−Borane Adducts: New Interest in Old Molecules. *Chem. Rev.* **2010**, *110* (7), 4023−4078.
(20) Clark, T. J.; Rodezno, J. M.; Clendenning, S. B.; Aouba, S.; Brodersen, P. M.; Lough, A. J.; Ruda, H. E.; Manners, I. Rhodium-catalyzed dehydrocoupling of fluorinated phosphine-borane adducts: synthesis, characterization, and properties of cyclic and polymeric phosphinoboranes with electron-withdrawing substituents at phosphorus. *Chem. - Eur. J.* **2005**, *11*, 4526−4534.
(21) Schäfer, A.; Jurca, T.; Turner, J.; Vance, J. R.; Lee, K.; Du, V. A.; Haddow, M. F.; Whittell, G. R.; Manners, I. Iron-Catalyzed Dehydropolymerization: A Convenient Route to Poly(phosphinoboranes) with Molecular-Weight Control. *Angew. Chem., Int. Ed.* **2015**, *54*, 4836−4841.
(22) Dorn, H.; Rodezno, J. M.; Brunnhöfer, B.; Rivard, E.; Massey, J. A.; Manners, I. Synthesis, Characterization, and Properties of the Polyphosphinoboranes [RPH−BH2]n (R = Ph, iBu, p-nBuC6H4, p-dodecylC6H4): Inorganic Polymers with a Phosphorus−Boron Backbone. *Macromolecules* **2003**, *36*, 291−297.
(23) Lai, X.; Zeng, X.; Li, H.; Zhang, H. Effect of Polyborosiloxane on the Flame Retardancy and Thermal Degradation of Intumescent Flame Retardant Polypropylene. *J. Macromol. Sci., Part B: Phys.* **2014**, *53* (4), 721−734.
(24) Joseph, P.; Tretsiakova-Mcnally, S. Reactive modifications of some chain- and step-growth polymers with phosphorus-containing compounds: effects on flame retardance—a review. *Polym. Adv. Technol.* **2011**, *22*, 395−406.
(25) Hooper, T. N.; Weller, A. S.; Beattie, N. A.; Macgregor, S. A. Dehydrocoupling of phosphine−boranes using the [RhCp*Me(PMe3)(CH2Cl2)][BArF4] precatalyst: stoichiometric and catalytic studies. *Chem. Sci.* **2016**, *7*, 2414−2426.
(26) Gamble, E. L.; Gilmont, P. Preparation and Properties of Diborane Diphosphine. *J. Am. Chem. Soc.* **1940**, *62* (4), 717−721.
(27) Rudolph, R. W.; Parry, R. W.; Farran, C. F. The Structure of Phosphine Borane. *Inorg. Chem.* **1966**, *5* (5), 723−726.
(28) Muetterties, E. L. *The Chemistry of Boron and Its Compounds*; Wiley: New York, 1967.
(29) Dorn, H.; Singh, R. A.; Massey, J. A.; Lough, A. J.; Manners, I. Rhodium-catalyzed formation of phosphorus-boron bonds: Synthesis of the first high molecular weight poly(phosphinoborane). *Angew. Chem., Int. Ed.* **1999**, *38* (22), 3321−3323.
(30) Dorn, H.; Singh, R. A.; Massey, J. A.; Nelson, J. M.; Jaska, C. A.; Lough, A. J.; Manners, I. Transition Metal-Catalyzed Formation of Phosphorus-Boron Bonds: A New Route to Phosphinoborane Rings, Chains, and Macromolecules. *J. Am. Chem. Soc.* **2000**, *122*, 6669−6678.
(31) Turner, J. R.; Resendiz-Lara, D. A.; Jurca, T.; Schäfer, A.; Vance, J. R.; Beckett, L.; Whittell, G. R.; Musgrave, R. A.; Sparkes, H. A.; Manners, I. Synthesis, Characterization, and Properties of Poly(aryl)-phosphinoboranes Formed via Iron-Catalyzed Dehydropolymerization. *Macromol. Chem. Phys.* **2017**, *218*, 1700120.
(32) Pandey, S.; Lönnecke, P.; Hey-Hawkins, E. Phosphorus−Boron-Based Polymers Obtained by Dehydrocoupling of Ferrocenylphosphine−Borane Adducts. *Eur. J. Inorg. Chem.* **2014**, *2014*, 2456−2465.
(33) Huertos, M. A.; Weller, A. S. Revealing the P−B coupling event in the rhodium catalysed dehydrocoupling of phosphine−boranes H3B·PR2H (R = tBu, Ph). *Chem. Sci.* **2013**, *4*, 1881−1888.
(34) Marquardt, C.; Jurca, T.; Schwan, K.-C.; Stauber, A.; Virovets, A. V.; Whittell, G. R.; Manners, I.; Scheer, M. Metal-Free Addition/Head-to-Tail Polymerization of Transient Phosphinoboranes, RPH-BH2: A Route to Poly(alkylphosphinoboranes). *Angew. Chem., Int. Ed.* **2015**, *54*, 13782−13786.
(35) Porter, D. *Group Interaction Modelling of Polymer Properties*; Marcel Dekker: New York, 1995.
(36) Dehghan, M.; Al-Mahaidi, R.; Sbarski, I. Investigation of CNT Modification of Epoxy Resin in CFRP Strengthening Systems. *Polym. Compos.* **2016**, *37* (4), 1021−1033.
(37) Cornille, A.; Auvergne, R.; Figovsky, O.; Boutevin, B.; Caillol, S. A perspective approach to sustainable routes for non-isocyanate polyurethanes. *Eur. Polym. J.* **2017**, *87*, 535−552.
(38) Petr, M.; Katzman, B.; DiNatale, W.; Hammond, P. T. Synthesis of a New, Low-Tg Siloxane Thermoplastic Elastomer with a Functionalizable Backbone and Its Use as a Rapid, Room Temperature Photoactuator. *Macromolecules* **2013**, *46* (7), 2823−2832.
(39) Hearley, A. K.; Nowack, R. J.; Rieger, B. New Single-Site Palladium Catalysts for the Nonalternating Copolymerization of Ethylene and Carbon Monoxide. *Organometallics* **2005**, *24*, 2755−2763.
(40) Giordano, G.; Crabtree, R. H. Di-μ-Chloro-Bis(η4−1,5-Cyclooctadiene) Dirhodium(I). *Inorg. Synth.* **1979**, *19*, 218−220.
(41) Tavtorkin, A. N.; Toloraya, S. A.; Nifant'ev, E. E.; Nifant'ev, I. E. A new method for the synthesis of dichlorophosphines. *Tetrahedron Lett.* **2011**, *52* (7), 824−825.
(42) Paul, U. S. D.; Braunschweig, H.; Radius, U. Iridium-catalysed dehydrocoupling of aryl phosphine−borane adducts: synthesis and characterisation of high molecular weight poly(phosphinoboranes). *Chem. Commun.* **2016**, *52*, 8573−8576.
(43) Hurtado, M.; Yánez, M.; Herrero, R.; Guerrero, A.; Dávalos, J. Z.; Abboud, J.-L. M.; Khater, B.; Guillemin, J.-C. The ever-surprising chemistry of boron: enhanced acidity of phosphine.boranes. *Chem. - Eur. J.* **2009**, *15*, 4622−4629.

DOI: 10.1021/acs.macromol.7b02030
Macromolecules 2017, 50, 9239−9248

(44) Mezger, T. G. *The Rheology Handbook: For Users of Rotational and Oscillatory Rheometers*, 2nd ed.; Vincentz Network GmbH & Co KG.: Hannover, 2006.
(45) van Krevelen, D. W. *Properties of Polymers*, 3rd ed.; Elsevier: Amsterdam, 1993.

DOI: 10.1021/acs.macromol.7b02030
Macromolecules 2017, 50, 9239−9248

Primary alkyl phosphine-borane polymers: Synthesis, low glass transition temperature, and a predictive capability thereof

Cavaye, H.

2017-11-30

Cavaye H, Clegg F, Gould PJ, et al., (2017) Primary alkyl phosphine-borane polymers: Synthesis, low glass transition temperature, and a predictive capability thereof. Macromolecules Volume 50, Issue 23, November 2017, pp. 9239-9248

https://doi.org/10.1021/acs.macromol.7b02030